Krieg (1973) has studied one-dimensional constant strain elements for the numerical solution of the one-dimensional wave (Helmholtz) equation. In this work, the dependence of the mass matrix approximation and temporal discretization was studied on the accuracy of the numerical solution. Belytschko and Mullen (1978) extended their dispersion analysis to higher (quadratic) order one-dimensional elements. It was shown that an optical branch in the spectrum exists. In the Brillouin's book (Brillouin, 1953), the lowest branch is called the *acoustic* while the higher branches are known as *optical* ones. The existence of optical branches causes the presence of the noise associated with the propagation of discontinuities. In the above mentioned study, the dispersion analysis revealed the existence 'stopping' bands in the frequency spectrum of quadratic elements, where solution in the frequency range decay exponentially. Also, the dispersion analysis for Newmark's method (Newmark, 1959) and for central difference method (Dokainish and Subbaraj, 1989) together with the consistent and lumped mass matrix was explained. It was shown that the dispersion curves for both mentioned time numerical schemes depend on the value of the time integration step. On the basis of this analysis it was recommended, that the Newmark's method is suitable with consistent mass matrix while the central difference method with lumped mass matrix.

Holmes and Belytschko (1976) numerically showed, than the different mesh size produces the interior reflection contributing to propagation of the spurious waves. In their works (Bažant, 1978; Bažant and Celep, 1982) have analytically analyzed the magnitudes of the spurious reflections of this interior reflection. Celep and Bažant (1983) have showed, than the transitional domain does not absorb the occurrence of the spurious waves. One-dimensional Lagrangian and Hermitian elements have also been studied by Okrouhlík and Höschl (1993). The response of the one-dimensional constant strain element mesh on the Heaviside loading oscillation have been solved in (Jiang and Rogers, 1990) and the stress oscillation and propagation of the spurious waves have been described. It has been proved, that in principle the spurious oscillations can not be removed but only minimized to a certain extent. The stress amplitude of spurious oscillations depends only on the number of the finite elements through which the elastic wave has passed. The effects of mass matrix formulation, time integrations and various combinations on the dispersion properties of the one-dimensional constant strain element have been presented, see (Goudreau and Taylor, 1972; Hughes, 1983; Hughes and Tezduyar, 1984). For many finite element types, their geometries and direct time integration schemes their dispersion properties are derived and described in many papers. On the other hand, a little attention has been so far paid to the study of the response of the finite element mesh to a loading by means of Heaviside step function.

This paper intends to study of the influence of the spatial discretization by finite element method on the accuracy of the wave propagation problem. The accuracy and dispersion analysis will be carried out for higher order classical and spectral finite elements (Patera, 1984), (Sprague and Geers, 2008) employed for the study of one-dimensional elastic wave propagation. Spectral elements are of h-type formulation with special positions of the nodes. The nodal positions are chosen in the agreement with employed the quadrature scheme. In this paper, the Legendre and Chebyshev spectral elements will be studied. The Legendre spectral element has nodal positions corresponding to the Gauss-Lobatto-Legendre quadrature (GLL), Chebyshev spectral element is associated with the Gauss-Lobbato-Chebyshev quadrature scheme (GLC) and, of course, the displacements along the element is approximated by Lagrangian interpolation functions (Atkinson, 1988). For these shape functions with corresponding quadrature formula, the mass matrix is evidently diagonal. In the seismology community, the spectral elements are very

popular for their small dispersion errors and marginal anisotropy effects (Cohen, 2002). The response of the elastic bar on the force loading by Heaviside step function will be studied in the close form for the continuous time and the stress field will be compared with the analytical solution (Kolsky and Key, 1963). After the time continuous numerical solution of the shock wave propagation in the discretized system is found, the results of the spatial dispersion analysis can be mutually compared and the numerical parasitic effects can be explained. For the shock loading, the stress and velocity field proves the jump in the wavefront propagated by wave speed. For this reason, the oscillation near the wavefront in the finite element solution is existing (Gibb's effect) and this effect will be investigated. The response of a 'thin' elastic bar will be studied by various types of finite element approaches. For the practical FE using for the wave propagation problems, the error estimation is necessary to accomplish and determine of the properties of the numerical solution and further, investigate the recommendation on the 'reliable' numerical model.

2. Problem formulation

The analytical solution of the response a one-dimensional 'thin' bar (Fig.1) under the loading will be derived for following assumptions: small strains, small displacements and rotations and linear constitutive equation in the form of Hooke's law. The transverse contraction of a cross-section of the bar is neglected. The one-dimensional wave equation in elastic solid continuum has the form, see e.g. (Kolsky and Key, 1963),

$$A\rho\frac{\partial^2 u}{\partial t^2} = AE\frac{\partial^2 u}{\partial x^2}, \tag{1}$$

where $u(x,t)$ is axial displacement, $x \in <0, L>$ is axial coordinate, L is length of a bar, t denotes time, ρ is mass density, A is area of a cross-section and E denotes Young's modulus. The wave speed in the bar is

$$c_0 = \sqrt{E/\rho}. \tag{2}$$

For the solution of (1) the boundary and initial conditions are to be defined. The right-hand side of the bar is fixed. So, the boundary conditions is are

$$u(x = L, t) = 0, \quad v(x = L, t) = 0, \quad t \in <0, \infty). \tag{3}$$

The initial conditions are defined by

$$u(x, t = 0) = 0, \qquad v(x, t = 0) = 0, \quad x \in <0, L>, \tag{4}$$

where v denotes velocity, e.g. $v = \frac{du}{dt}$.

The loading by a force applied at the free end of the bar leads to

$$F(t) = A\sigma(x = 0, t) = AE\frac{\partial u(x = 0, t)}{\partial x}, \tag{5}$$

where the time dependence of stress σ is given by Heaviside step function $H(t)$ in the form

$$\sigma(x = 0, t) = \sigma_0 H(t), \tag{6}$$

where $\sigma_0 = F_0/A$. Heaviside step function $H(t)$ is defined as

$$H(t < 0) = 0, \qquad H(t \geq 0) = 1. \tag{7}$$

The properties of Heaviside step function $H(t)$ can see in (Kanwal, 1998).

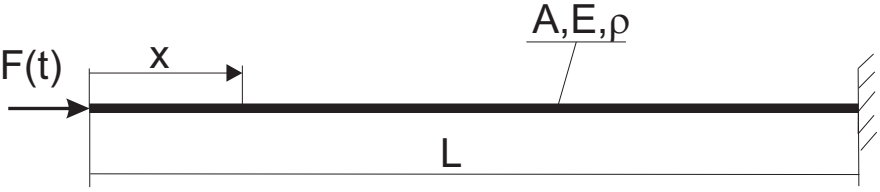

Figure 1: One-dimensional bar under force loading.

3. FEM discretization

Consider the finite element approximation of the solution (Hughes, 1983)

$$u^e(\xi) = \sum_{i=1}^{p+1} h_i(\xi) u_i^e, \quad \xi \in < -1, 1 > \tag{8}$$

where $h(\xi)$ are shape functions defined in the local element coordinates ξ, and p is the spectral order (polynomial order), u_i^e are nodal displacements. In matrix formulation we have

$$u^e(\xi) = \mathbf{H}(\xi)\mathbf{u}^e, \tag{9}$$

where $\mathbf{u}^e$ denotes local nodal displacement vector for given element.

Spatial discretization by the finite element of elastodynamics problems leads to the ordinary differential system

$$\mathbf{M}\ddot{\mathbf{u}} + \mathbf{K}\mathbf{u} = \mathbf{R}. \tag{10}$$

Here, $\mathbf{M}$ is the mass matrix, $\mathbf{K}$ the stiffness matrix, $\mathbf{R}$ is the time-dependent load vector, and $\mathbf{u}$ and $\ddot{\mathbf{u}}$ contain nodal displacements and accelerations. The element mass and stiffness matrices are given by

$$\mathbf{M}^e = \int_{L^e} \rho \mathbf{H}^T \mathbf{H} \, \mathrm{d}x \tag{11}$$

and

$$\mathbf{K}^e = \int_{L^e} E \mathbf{B}^T \mathbf{B} \, \mathrm{d}x \tag{12}$$

where L^e denotes the element length, $\mathbf{B}$ is the strain-displacement matrix, $\mathbf{H}$ stores the displacement interpolation functions h_i and integration is carried over the element domain. Global matrices are assembled in the usual fashion. Mass matrix defined by (11) is called consistent mass matrix preserving the kinetic energy. The matrices given by (11) and (12) are real, symmetrical, their eigenvalues are real and non-negative.

A lot of direct time integration methods are known. The implicit (Subbaraj and Dokainish, 1989) and explicit (Dokainish and Subbaraj, 1989) methods are often used for the numerical solution in transient elastodynamics. The explicit methods often require the lumped (diagonal) mass matrix formulation (Hughes, 1983). In this paper, the row-sum method and HRZ scaling lumped mass algorithms (Hinton, Rock and Zienkiewicz, 1976) is employed.

3.1. Classical finite elements

For classical h-type FE the displacement approximation is realized by Lagrangian interpolation polynomials in the form (Hughes, 1983)

$$h_i(\xi) = \prod_{j \neq i} \frac{\xi - \xi_i}{\xi_j - \xi_i}, \quad \forall\, i, j \in \{1, 2, \ldots, p+1\}, \tag{13}$$

where nodal positions along the element $\xi_i, i = 1, 2, \ldots, p+1$ are chosen uniformly. The basic property of Lagrangian interpolants as shape functions is following

$$h_i(\xi_j) = \delta_{ij}, \tag{14}$$

where δ_{ij} is Kronecker delta. This concept of FE interpolation produces the C^0 continuous weak solution.

In classical FEM, the integral (11) and (12) are evaluated with Gauss-Legendre quadrature formula (Irons, 1966) with linear mapping range $x \in (x_j, x_j + L_j^e), j = 1, 2, \ldots, NELEM$ to range $\xi \in < -1, 1 >$, where the intergation points are the roots of the Legendre polynomial of a given degree. $NELEM$ is number of finite elements in one-dimensional mesh. Generally, the quadrature of Gauss type on the range $\xi \in < -1, 1 >$ is given by

$$\int_{-1}^{1} f(\xi)\, \mathrm{d}\xi = \sum_{i=1}^{n} w_i f(\xi_i), \tag{15}$$

where $\xi_i, i = 1, 2, \ldots, n$ are the integration points and w_i are the corresponding weights. The table of the Gauss-Legendre points and corresponding weights is presented in (Atkinson, 1988).

3.2. Legendre spectral finite elements

As it was mentioned, the spectral FE is h-type FE with a special choice of the nodal positions according to the quadrature formula. For the Legendre spectral FE, the nodal positions are evaluated at $p+1$ Gauss-Lobatto-Legendre (GLL) points, such that $\xi_1 = -1$ and $\xi_{p+1} = 1$, with the other points being obtained as the roots of the derivative of the Legendre polynomials. GLL points ξ_i and the corresponding weight factors w_i can be found in (Atkinson, 1988) or (Cohen, 2002). The basic property of the spectral FE is that the mass matrix evaluated by corresponding quadrature is diagonal. The proof can be found in (14).

3.3. Chebyshev spectral finite elements

The Chebyshev FE is based on the Gauss-Lobatto-Chebyshev (GLC) quadrature, where nodal positions, also evidently integration points, are given by $\xi_i = -\cos\frac{(i-1)\pi}{p}, i = 1, 2, \ldots, p+1$ and the corresponding weights are identical and equal to $w_i = 2/(p+1)$, see e.g. (Atkinson, 1988).

4. Solution of motion equations

Analytical solution of the motion equations (10) can be found in the close form, where the time distributions of displacements, velocities, stresses are continuous. The response of the bar (undamped, nongyroscopic discrete system) under the step jump force loading (Fig.1) prescibed by equations (10) can be found by the convolution (Duhamel's) integral (Meirovitch, 1980).

Before the solution itself, the diagonalization of (10) is required. Using modal transformation we get

$$\mathbf{u} = \mathbf{V}\mathbf{q}, \tag{16}$$

where $\mathbf{q}$ is the vector of modal coordinates, the modal matrix $\mathbf{V}$ stores the eigenvectors in such a way $\mathbf{V} = [\Phi_i], i = 1, 2. \ldots, n$, n is degrees of freedom of system (10). Corresponding spectral matrix $\mathbf{\Lambda}$ stores the eigenvalues $\mathbf{\Lambda} = \mathrm{diag}(\omega_i^2)$ computed from the generalized eigenvalue problem

$$\omega_i^2 \mathbf{M}\mathbf{\Phi}_i + \mathbf{K}\mathbf{\Phi}_i = \mathbf{0}, \quad i = 1, n. \tag{17}$$

If the spectral and modal matrices are normalized by relationships

$$\mathbf{V}^{\mathrm{T}}\mathbf{M}\mathbf{V} = \mathbf{I}, \quad \mathbf{V}^{\mathrm{T}}\mathbf{K}\mathbf{V} = \mathbf{\Lambda}, \tag{18}$$

where $\mathbf{I}$ is the unit matrix, the system after the modal transformation (16) is diagonalized and yields a system of the second order ode's equations

$$\ddot{\mathbf{q}}(t) + \mathbf{\Lambda}\mathbf{q}(\mathbf{t}) = \mathbf{N}(\mathbf{t}), \tag{19}$$

where vector $\mathbf{N}(t)$ is given by

$$\mathbf{N}(t) = \mathbf{V}^{\mathrm{T}}\mathbf{F}(t). \tag{20}$$

The equation (19) represents a set of independent ode's having the form

$$\begin{aligned} \ddot{q}_i &= N_i(t), \qquad i = 1, 2, \ldots, r, \\ \ddot{q}_i + \omega_1^2 q_i &= N_i(t), \qquad i = r+1, r+2, \ldots, N. \end{aligned} \tag{21}$$

where r denotes the number of rigid-body modes ($\omega_i = 0$ for $i = 1, 2, \ldots, r$), in the process, $n-r$ is the number of elastic modes. The close form solution of (19) can be found by convolution integral. For the homogeneous initial conditions it yields the solution

$$\begin{aligned} q_i(t) &= \int_0^t \left[\int_0^\tau N_i(\eta)\, \mathrm{d}\eta \right] \mathrm{d}\tau, \qquad i = 1, 2, \ldots, r, \\ q_i(t) &= \frac{1}{\omega_i} \int_0^t N_i(t-\tau) \sin \omega_i \tau \, \mathrm{d}\tau, \quad i = r+1, r+2, \ldots, n. \end{aligned} \tag{22}$$

For the configuration given by Fig.1, the time dependence loading vector $\mathbf{R}$ is a constant-value vector for time $t \geq 0$

$$\mathbf{R}(t) = [F_0, 0, 0, \ldots, 0, 0]^{\mathrm{T}}, \tag{23}$$

where the force F_0 is applied on the global node u_1 for $x = 0$. If the boundary conditions (3) are applied, the all eigenvalues are positive. Therefore, the motion in the rigid mode is eliminated. If the eigenvalue problem (17) is solved for the prescribed boundary conditions (3) and the eigenfrequencies are sorted in increasing order, then the spectral matrix has the form

$$\mathbf{\Lambda} = \mathrm{diag}\left(\omega_1^2, \omega_2^2, \ldots, \omega_{n-1}^2, \omega_n^2\right), \quad n = NELEM - 1. \tag{24}$$

Of course, from (16) and (23), the components of the vector $\mathbf{N}(t)$ is constant-value

$$\mathbf{N}(t) = [N_1, N_2, \ldots, N_{n-1}, N_n]^{\mathrm{T}} \tag{25}$$

and the convolution integral of (21) can be simply computed by

$$q_i = \frac{1}{\omega_i} \int_0^t N_i \sin \omega_i \tau \, \mathrm{d}\tau = \frac{N_i}{\omega_i} \left(1 - \cos \omega_i t\right), \qquad i = 2, 3, \ldots, n. \tag{26}$$

Sequentially, the nodal displacement vector $\mathbf{u}$ for given time t is than established by relationship (16), it is in series form. Further, the nodal velocity vector is given by

$$\dot{\mathbf{u}} = \mathbf{V}\dot{\mathbf{q}}, \tag{27}$$

where

$$\dot{q}_i = \frac{N_i}{\omega_i} \sin \omega_i t, \qquad i = 2, 3, \ldots, n. \tag{28}$$

And finally, the approximation of stress distribution along the bar is prescribed by means of the strain-displacement matrix $\mathbf{B}$ and Hooke's law in the form

$$\boldsymbol{\sigma} = E\mathbf{B}\mathbf{u}. \tag{29}$$

Frequently, the stress values are computed at integration points and consecutively recomputed to nodes.

5. Dispersion of classical and spectral FE

In work of Thompson and Pinsky (1994), the complex wavenumber dispersion analysis was presented for the one-dimensional FE. For arbitrary spectral order p, the computational approach using the symbolic operations is very simple to implement. In the Fourier analysis, the nodal displacements are prescribed in the form

$$u_i = A_i \exp(\mathrm{i}\omega t) \exp(\mathrm{i}k^h x_i), \tag{30}$$

where the discrete wavenumber is the real part of k^h and imaginary part of k^h has the meaning the attenuation intensity, imaginary unit $\mathrm{i} = \sqrt{-1}$ and x_i is the nodal position. Next, the relationship (30) is substituted into (10) and the dispersion relation $\omega = f(k^h)$ is obtained. In this paper, the dispersion branches are depicted in the half of the first Brillouin's zone $Re(k^h L^e) \in < 0, \pi >$, see (Brillouin, 1953).

In Figs. 2 to 6 the dispersion realitions are presented for the classical FE with consistent and diagonal mass matrix by row-sum method and by HRZ algorithms, respectively, and for Legendre and Chebyshev spectral FE, where spectral order is $p = 1, 2, 3$. Note, that the linear spectral FE corresponds to the classical linear FE with lumped mass matrix.

It can be seen, that the higher classical FE produces smaller dispersion errors in the lower dispersion branches. The odd spectral order p is recommended due to minimal range of stopping bands. This property of dispersion behaviour is valid for the Legendre FE, simultaneous diagonal mass matrix as well. On the other side, the dispersion of Chebyshev FE is unsatisfactory, because the diagonal parts of global mass matrix corresponding to the exterior nodes of elements have double value of the interior node mass coefficients.

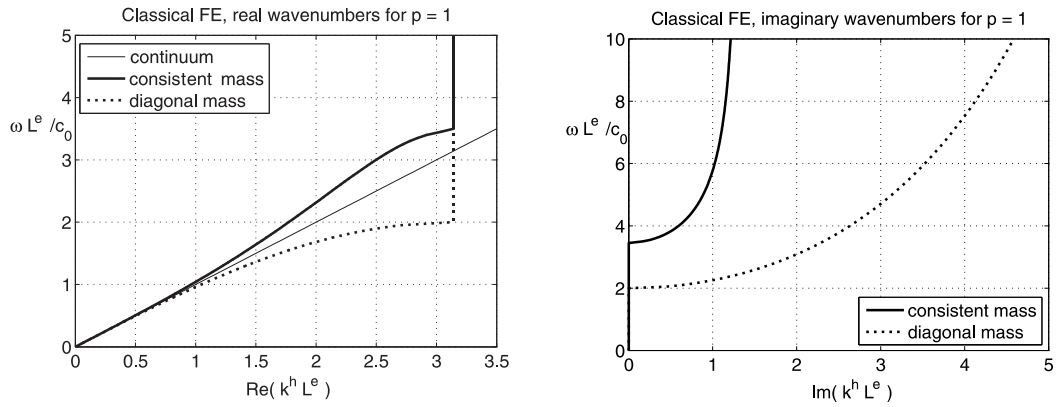

Figure 2: Frequency spectrum for linear (p=1) classical FE. Real wavenumbers (on the left), imaginary wavenumbers (on the right).

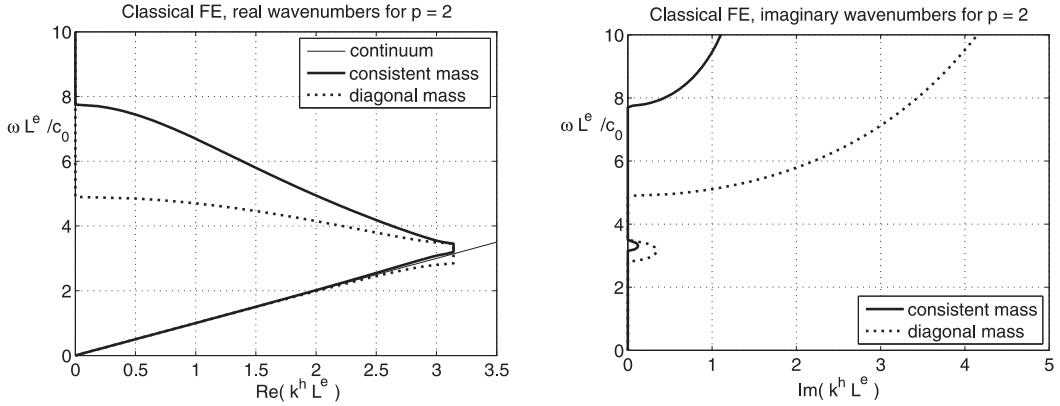

Figure 3: Frequency spectrum for quadratic (p=2) classical FE. Real wavenumbers (on the left), imaginary wavenumbers (on the right).

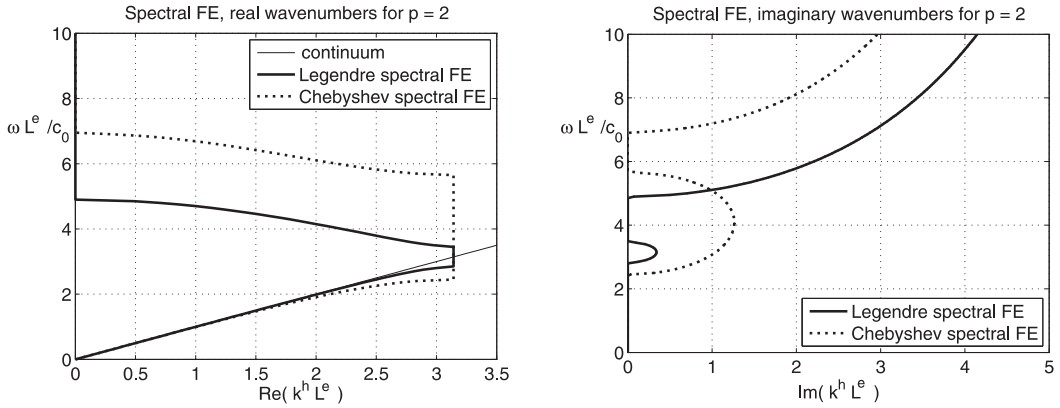

Figure 4: Frequency spectrum for quadratic (p=2) spectral FE. Real wavenumbers (on the left), imaginary wavenumbers (on the right).

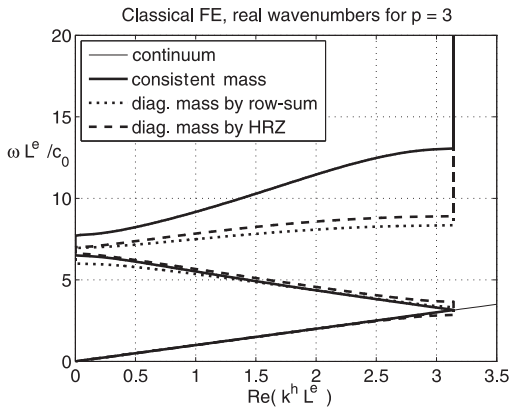

Figure 5: Frequency spectrum for cubic (p=3) classical FE. Real wavenumbers (on the left), imaginary wavenumbers (on the right).

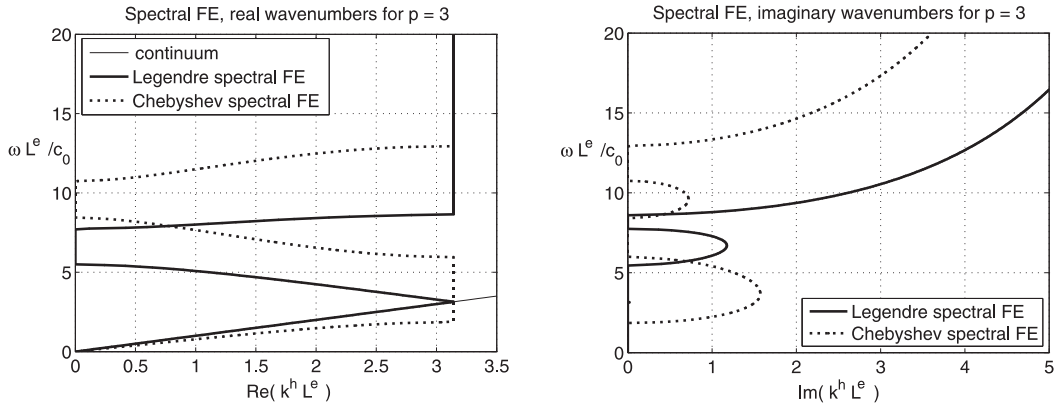

Figure 6: Frequency spectrum for quadratic (p=3) spectral FE. Real wavenumbers (on the left), imaginary wavenumbers (on the right).

6. Fourier spectrum of Heaviside pulse

For the given time distribution of the loading, its spectrum can be determined by Fourier's analysis. The amplitude density for the rectangle pulse with amplitude F_0 and duration time $t \in (0, T)$ is prescribed by

$$\frac{A(\omega)}{\pi F_0 T} = \left(\frac{2}{\pi^2}\right) \left| \frac{\sin \frac{\omega T}{2}}{\frac{\omega T}{\pi}} \right| . \tag{31}$$

This relation for the amplitude density of the rectangle pulse shown in Fig.7. The spectrum for given T can be used for the analysis frequency range and dispersion spectrum of FE.

7. Results

The results of the problem defined in Sec. 2. and solved in the close form in Sec. 4. are presented in this section. The amplitude of the loading force $F(t)$ by Heaviside step function is denoted F_0, therefore the stress wave with the nominal axial stress $\sigma_0 = F_0/A$ is generated and the corresponding speed of movement of a particle has value $v_0 = \sigma/(\rho c_0)$. The nondimensional

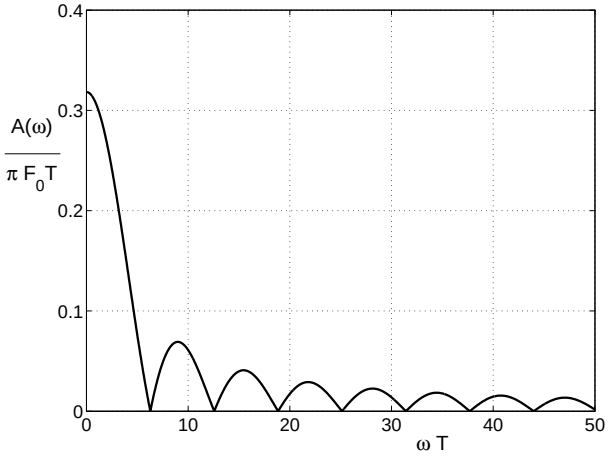

Figure 7: Amplitude density of rectangle pulse during time T.

axial stress σ/σ_0 will be depicted along the bar as the function nondimensional axial coordinate x/L. The response of the elastic bar for the different types of FE is presented for time $t/t_0 = 1/2$, where $t_0 = L/c_0$ is the nondimensional time needed for the wave to pass through the bar. This time is chosen to eliminate wave reflections at the end of the bar.

The analytical solution of this wave propagation problem by classical theory was introduced in (Kolsky and Key, 1963). The analytical solution will be used for assesing of the influence of the FE type and spectral order on the stress state. In the following text, the bar of length L is discretizated by fifty classical and spectral finite elements, $NELEM = 50$.

7.1. Classical FE

The response of the bar discretizated by classical linear finite elements, where consistent and diagonal mass matrices are assummed, is shown in Fig. 8. For the consistent mass matrix, the stress distribution oscillates especially in front of the theoretical wavefront. This is outcome of the dispersion analysis, where wave speed for linear element with consistent mass matrix is greater than the 'exact' wave speed value. On the other side, the stress distribution for the diagonal mass matrix oscillates in front of the theoretical wave front. It follows from the dispersion analysis, where wave speed is smaller than the 'exact' wave speed value. This is a generally known fact (Belytschko and Mullen, 1978).

The response for quadratic ($p = 2$) FE is shown in Fig. 9. The oscillations for quadratic FE have lower intensity than these for linear elements. The stress jump is well approximated and the wave speed effects for consistent and diagonal mass matrix are the same as those for linear elements. For the diagonal mass matrix, the spurious oscillations is not obvious in front of the wavefront, but they are not negligible in front of the wavefront. The diagonal mass matrix by row-sum method and by HRZ algorithms is the same.

For the higher order FE ($p = 3$ and $p = 5$), the intensity of the spurious oscillations is decreasing, see Fig. 10 and Fig.11. The diagonal mass matrix by row-sum method proves higher accuracy than the diagonal mass matrux given by HRZ algorithms.

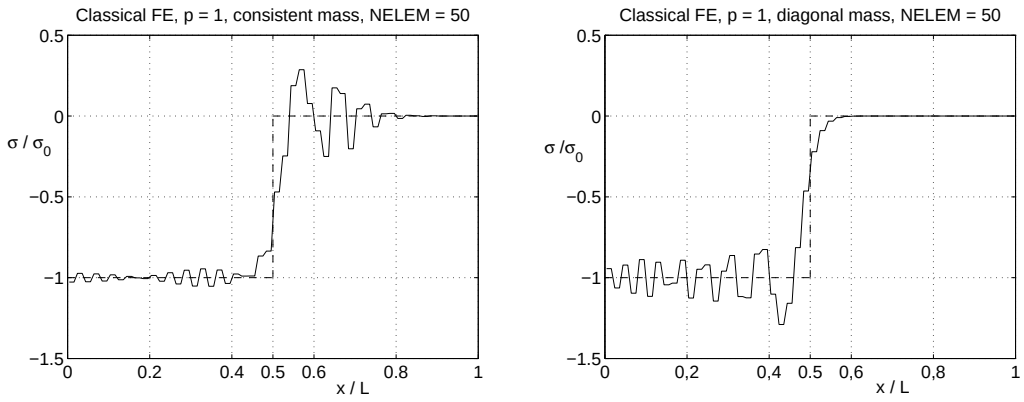

Figure 8: Stress distribution in a elastic bar for linear ($p = 1$) classical FE with consistent mass matrix (on the left) and with diagonal mass matrix (on the right) for time $t/t_0 = 1/2$.

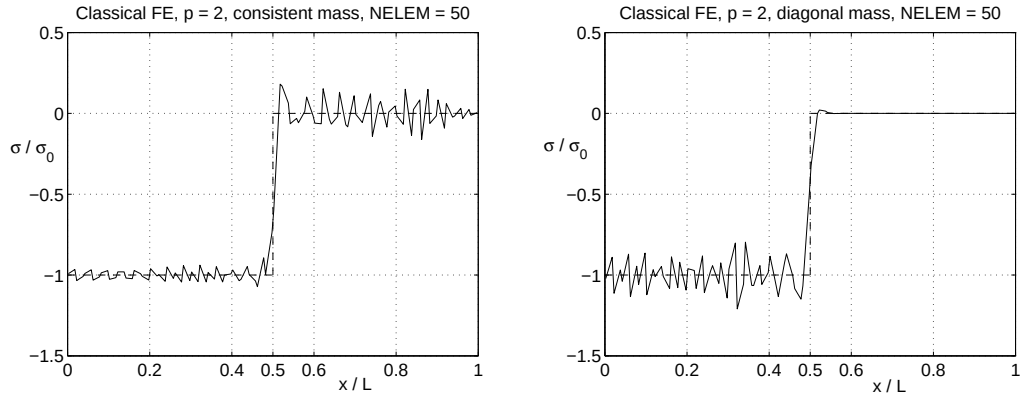

Figure 9: Stress distribution in a elastic bar for quadratic ($p = 2$) classical FE with consistent mass matrix (on the left) and with diagonal mass matrix (on the right) for time $t/t_0 = 1/2$.

7.2. Chebyshev spectral FE

The stress distribution for the quadratic spectral Chebyshev FE has the behaviour similar to the linear classical FE with diagonal mass matrix. On the other side, the higher spectral Chebyshev finite elements are not suitable for the numerical solution of wave propagation problems, see Fig. 12. This fact can be explained by unfavourable dispersion properties, see Fig. 6.

7.3. Legendre spectral FE

The higher order ($p = 3, 5$) Legendre spectral finite elements, where mass matrix is naturally diagonal, offer a very good choice for the numerical solution of the elastic wave propagation problems. The response of the bar for the cubic and quintic Legendre spectral FE is presented in Fig. 13, where spurious oscillations are smaller than those of the classical FE with diagonal mass matrix. The Legendre spectral FE have a potential for being employed in explicit elastodynamics, where the lumped mass matrix is required.

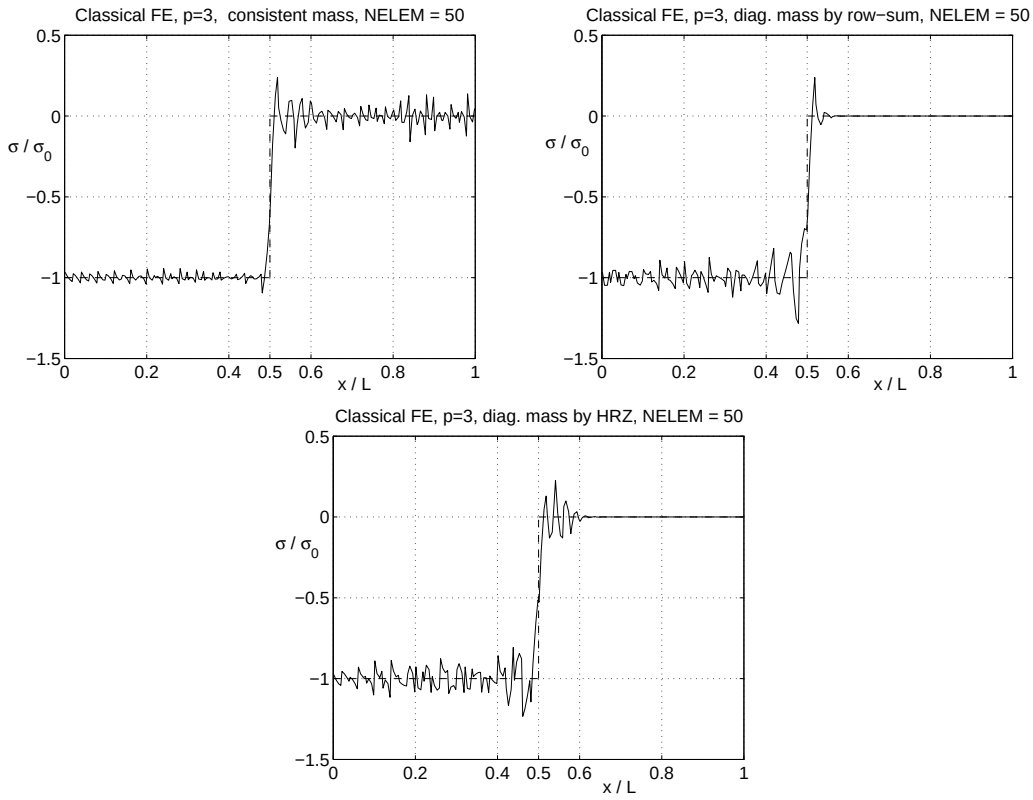

Figure 10: Stress distribution in a elastic bar for cubic ($p = 3$) classical FE with consistent mass matrix (on the left), with diagonal mass matrix by row-sum method (on the right) and with diagonal mass matrix by HRZ algorithms (on the bottom) for time $t/t_0 = 1/2$.

8. Conclusions

In this paper, the dispersion properties of different types of one-dimensional finite elements were studied. The attention has been paid to the classical finite elements and Legendre and Chebyshev spectral finite elements. Dispersion relations for different orders of approximation polynomials are presented. The spatial discretization by finite element method was studied in the one-dimensional wave propagation in the elastic 'thin' bar, where the loading was taken in the form of the Heaviside step function. The numerical solution by higher order classical and spectral finite elements were tested and compared with the solution by classical theory of elastic stress propagation. For the FE spatial discretization, the close form of analytical solution in the series form was found, where all eigenfrequencies are necessary to compute. Classical finite elements with consistent and diagonal mass matrix by row-sum method and HRZ algorithms was considered and also Legendre and Chebyshev spectral finite element were used. The Legendre spectral finite element method makes advantageous use of diagonal mass matrix with the preservation of the qood dispersion properties against classical finite element with lumped (diagonal) mass matrix. It was recommend to choose the odd spectral order ($p = 3, 5$) due to minimal stopping band range for the lower dispersion branches. The Legendre spectral element has a potential to the appropriate numerical solution of a elastic wave propagation problem with fractional encroachment to the standard finite element codes, where the nodal positions and the quadrature technique is changed. The spectral Legendre FEM produces diagonal mass matrix

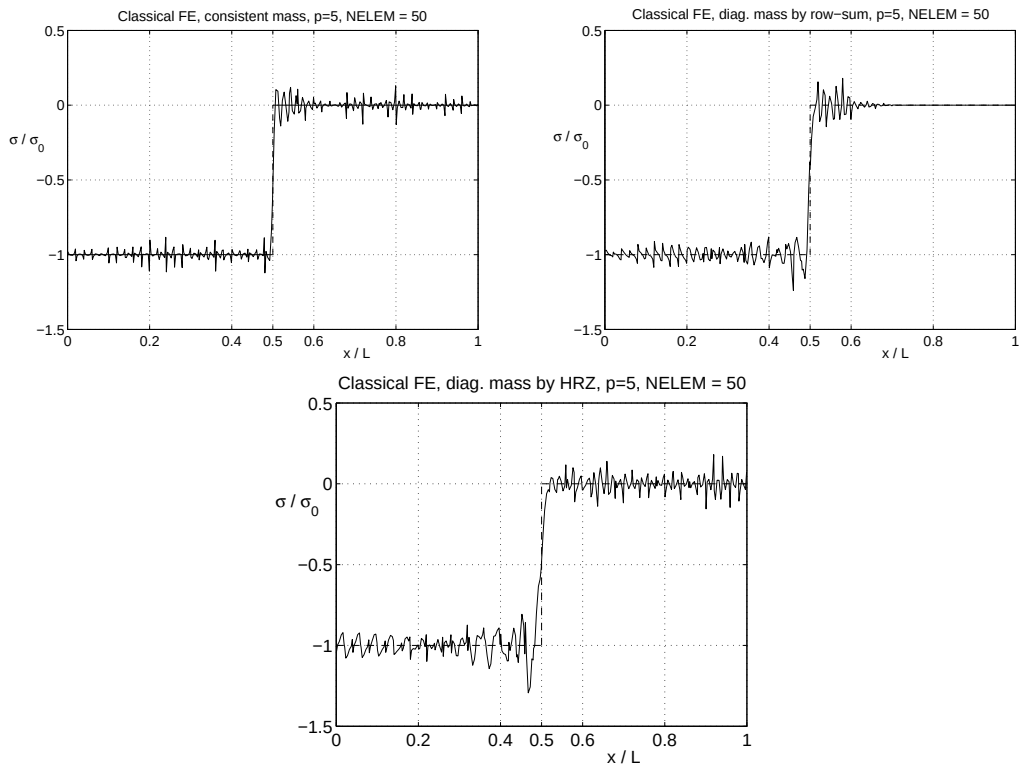

Figure 11: Stress distribution in a elastic bar for quintic ($p = 5$) classical FE with consistent mass matrix (on the left), with diagonal mass matrix by row-sum method(on the right) and with diagonal mass matrix by HRZ algorithms (on the bottom) for time $t/t_0 = 1/2$.

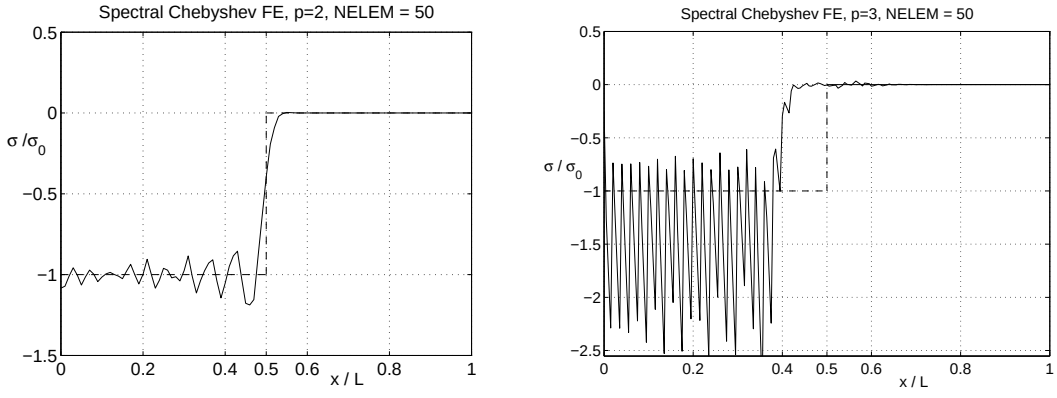

Figure 12: Stress distribution in a elastic bar for quadratic ($p = 2$) (on the left) and for cubic ($p = 3$) (on the right) spectral Chebyshev FE for time $t/t_0 = 1/2$.

needed to the explicit direct time integration. The Chebyshev spectral finite elements are not recommended for the computational elastic wave propagation due to their unsuible dispersion spectrum.

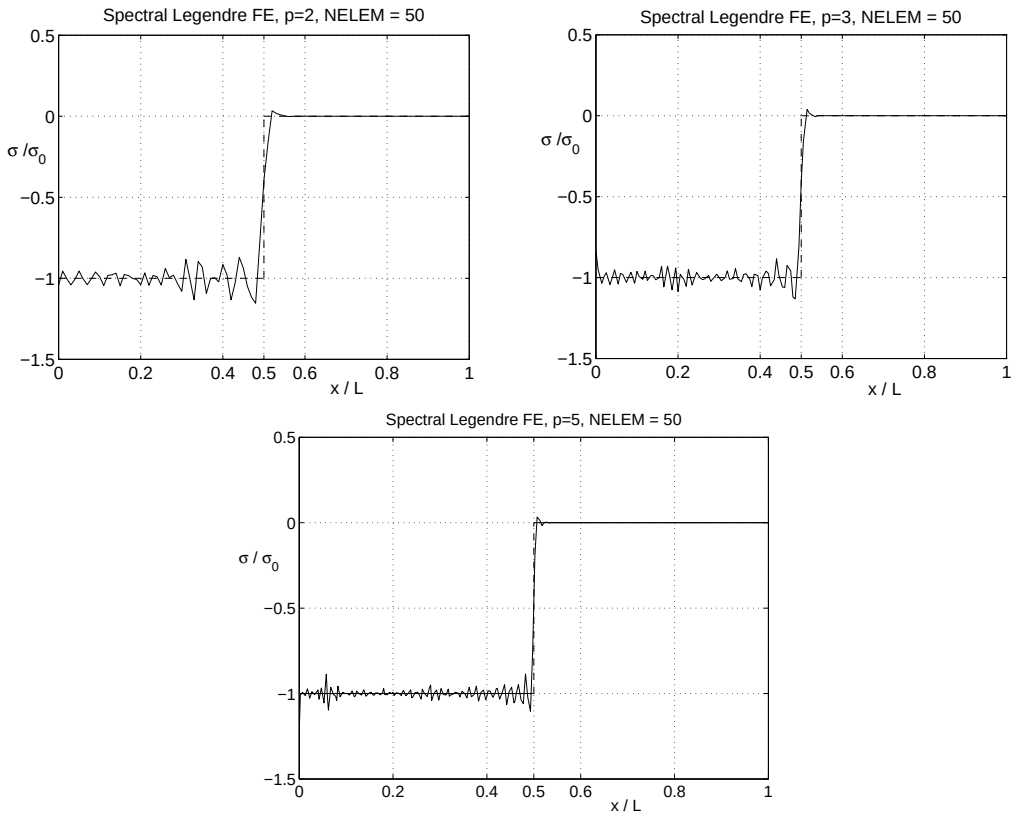

Figure 13: Stress distribution in a elastic bar for quadratic ($p = 2$) (on the left), for cubic ($p = 3$) (on the right) and for quintic ($p = 5$) (on the bottom) spectral Legendre FE for time $t/t_0 = 1/2$.

9. Acknowledgment

The support of grants GA ČR P101/10/P376, 101/09/1630 and 101/07/1471 under AV0Z20760514 is gratefully acknowledged.

10. References

Atkinson, K. E. 1988: *Introduction to Numerical Analysis.* John Wiley, Singapore.

Bažant, Z.P. 1978: Spurious reflection of elastic wave in nonuniform finite elements grids. *Computer Methods in Applied Mechanics and Engineering*, vol. 16, 91-100.

Bažant, Z.P. & Celep, Z. 1982: Spurious reflection of elastic wave in nonuniform mesh of constant and linear strain finite elements. *Computers & Structures*, vol. 15, 451-459, 1982.

Belytschko, T. & Mullen, R. 1978: On dispersive properties of finite element solutions. In *Modern Problems in Elastic Wave Propagation.* Miklowitz, J. et al. (Editors), John Wiley, New York, 67-82.

Brillouin, L. 1953: *Wave propagation in Periodic Structures: Electric Filters and Crystal Lattices.* New York: Dover Publications.

Celep, Z. & Bažant, Z.P. 1983: Spurious reflection of elastic waves due to gradually changing

finite element size. *International Journal for Numerical Methods in Engineering*, vol. 19, 631-646.

Cohen, G.C. 2002: *Higher-order numerical methods for transient wave equation.* Springer-Verlag, Scientific Computation.

Dokainish, M.A. & Subbaraj, K. 1989: A survey of direct time-integration methods in computational structural dynamics - I. Explicit methods. *Computers & Structures*, vol. 32(6), 1371-1386.

Goudreau, G.L. & Taylor, R.L. 1972: Evaluation of numerical integration methods in elastodynamics. *Computer Methods in Applied Mechanics and Engineering*, vol. 2, 67-97.

Hinton, E. & Rock, T.A. & Zienkiewicz, O.C. 1976: A note on mass lumping and related processes in the finite element method., *Internation Journal of Earthquake Enginnering and Structures Dynamics*, vol. 4, 245-249.

Holmes, N. & Belytschko, T. 1976: Postprocessing of finite element transient response calculations by digital filters. *Computers & Structures*, vol. 6, 211-216.

Hughes, T.J.R. 1983: *The Finite Element Method: Linear and Dynamic Finite Element Analysis.* New York: Prentice-Hall, Englewood Cliffs.

Hughes, T.J.R. & Tezduyar, T.E. 1984: Stability and accuracy analysis of some fully-discrete algoritms for the one-dimensional second-order wave equation. *Computers & Structures*, vol. 19, 665-668.

Chin, R.C.Y. 1975: Dispersion and Gibb's phenomenon associated with difference approximations to initial boundary-value problems. *J. Comp. Phys*, vol. 18, 233-247.

Irons, B.M. 1966: Engineering application of numerical integration in stiffness method. *AIAA Journal*, vol. 14, 2035-2037.

Jiang, L. & Rogers, R.J. 1990: Effects of spatial discretization on dispersion and spurious oscillations in elastic wave propagation. *International Journal for Numerical Methods in Engineering*, vol. 29, 1205-1218.

Kanwal, R.P. 1998: *Generalized Functions: Theory and Technique.* 2nd ed. Boston, MA: Birkhuser.

Kolsky, H., 1963: *Stress Wave in Solids.*, New York: Dover Publications.

Krieg, R.D. & Key, S.W. 1973: Transient shell response by numerical time integration. *International Journal for Numerical Methods in Engineering*, vol. 7, 273-286.

Meirovitch, L. 1980: *Computational methods in structural dynamics.* Merylan: Sijthoff & Noordhoff.

Newmark, N.M. 1959: A method of computation for structural dynamic. *Journal of the Engineering Mechanics Division*, vol. 85, 67-94.

Okrouhlík, M. & Höschl, C. 1993: A contribution to the study of dispersive properties of one-dimensional Lagrangian and Hermitian elements. *Computers & Structures*, vol. 49(5), 779-795.

Patera, A.T. 1984: A spectral element method for fluid dynamics: Laminar flow in a channel expansion. *Journal of Computational Physics*, vol. 54, 468-488.

Sprague, M.A. & Geers, T.L. 2008: Legendre spectral finite elements for structural dynamics analysis. *Communications in Numerical Methods in Engineering*, vol. 24(12), 1953-1965.

Subbaraj, K. & Dokainish, M.A. 1989: A survey of direct time-integration methods in computational structural dynamics - II. Implicit methods. *Computers & Structures*, vol. 32(6), 1387-1401.

Thompson, L.L. & Pinsky, P.M. 1994: Complex wavenumber Fourier analysis of the p-version finite element method. *Computational Mechanics*, vol. 13(4), 255-275.

Vichnevetsky, R. & Bowles, J.B. 1982: *Fourier analysis of numerical approximations of hyperbolic equations.* SIAM, Philadelphia, 1982.